scientific reports

Check for updates

OPEN

Hypoxic preconditioning modulates BDNF signaling to alleviate depression-like behaviors in mice and its whole transcriptome sequencing analysis

Lizhu Chen[1,6], Xujie Wang[1,6], Xiaoe Jia[1,3], Rengui Bade[1,2], Xiaolei Liu[1], Shuyuan Jiang[1], Yabin Xie[1,2], Wei Xie[1,2]✉, Manhai Gao[4]✉ & Guo Shao[1,5]

Depression, a neurological disorder triggered by stressful stimuli such as hypoxia, is associated with high morbidity and mortality. Hypoxic preconditioning (HPC) is an endogenous mechanism that has been used in recent research to upregulate BDNF, a marker of depression, to elicit neuroprotective effects. However, the mechanisms by which HPC protects against depression remain poorly understood. Therefore, this study aimed to investigate the effects of HPC on depressive behaviors via BDNF signaling. Initially, ICR mice were subjected to HPC, followed by the establishment of a 24-hour restraint stress model to mimic depressive behaviors. Subsequent analysis focused on changes in depressive behaviors, biochemical markers, and the levels of BDNF and its ability to modulate synaptic structure and neurogenesis. Furthermore, whole transcriptome sequencing was conducted. The results indicated that HPC relieved characteristic depressive behaviors in restraint stress model mice, regulated neurotransmitter levels, elevated antioxidant capacity, and promoted BDNF signaling in the hippocampus. PSD-95 expression, the number and complexity of neuronal dendritic spines, and hippocampal neurogenesis in model mice were increased via HPC. Restraint stress regulated 373 DElncRNAs, 166 DEcircRNAs, 29 DEmiRNAs and 1235 DEmRNAs, which were also modulated by HPC. The ceRNA networks were constructed on the basis of these DERNAs. Functional enrichment analysis revealed that these genes are related to synapses, neurogenesis and neurotrophin signaling. These results suggested that HPC upregulated BDNF and activated BDNF/PLCγ/CREB signaling to alleviate synaptic deficits and promote hippocampal neurogenesis, ultimately ameliorating depressive behaviors in mice. The identification of various mRNAs and ncRNAs and their constituent ceRNAs provides theoretical guidance for the clinical treatment of depression with HPC.

Keywords Hypoxic preconditioning, Depression, Brain-derived neurotrophic factor, BDNF/TrkB signaling, Whole transcriptome sequencing

Major depressive disorder (MDD) is a prevalent mental illness characterized by severe mood disturbances and physiological dysfunction, often resulting in disability and suicide[1], and is predicted to become the leading global cause of disease by 2030[2]. However, a considerable number of MDD patients do not respond to traditional antidepressants. Nonpharmacological therapies such as repetitive transcranial magnetic stimulation may have long treatment durations and cycles[3]. Hence, the quest for novel and effective prevention and treatment strategies for MDD, along with understanding the brain mechanisms involved, remains a critical clinical challenge.

[1]Inner Mongolia Key Laboratory of Hypoxic Translational Medicine, Baotou Medical College, Baotou 014060, China. [2]School of Medical Technology and Anesthesia, Baotou Medical College, Baotou 014060, China. [3]School of Basic Medicine and Forensic Sciences, Baotou Medical College of Neuroscience Institute, Baotou Medical College, Baotou 014060, China. [4]Department of Anaesthesiology, The First Affiliated Hospital of Baotou Medical College, Baotou 014060, China. [5]Center for Translational Medicine, Department of Laboratory Medicine, The Third People's Hospital of Longgang District, Shenzhen 518112, China. [6]These authors contributed equally: Lizhu Chen and Xujie Wang. ✉email: xiewei@tmu.edu.cn; gaomanhaimazuike@163.com

Hypoxia is a common stress state in physiological and pathological processes and is implicated in the development of depression[4]. Hypoxic preconditioning (HPC) is an adaptive response to hypoxia, where repeated sublethal hypoxic stimuli make tissues or cells tolerant to subsequent lethal hypoxic stimuli[5,6]. HPC has been shown to have neuroprotective, antidepressant and anxiolytic effects in animal models of depression and MDD patients[7–9]. Notably, the protective effects of HPC are endogenous, unlike those of medication or surgery. However, the specific effects of HPC on depression and the molecular mechanisms are not yet fully understood.

Brain-derived neurotrophic factor (BDNF) is a chief molecular marker of depression. Reduced BDNF expression in the serum and brain tissue of depression patients is associated with impaired synaptic plasticity in the hippocampus, leading to hippocampal atrophy and subsequent neurological and behavioral abnormalities[10]. Common antidepressant drugs such as selective serotonin reuptake inhibitors (SSRIs) work by restoring BDNF levels[11]. Interestingly, our research indicates that HPC may exert neuroprotective effects by increasing BDNF expression[12], suggesting a potential role for HPC in alleviating depression through the modulation of BDNF expression.

The binding of brain-derived neurotrophic factor (BDNF) to the tropomyosin-related kinase B (TrkB) receptor initiates BDNF/TrkB signaling, which is related to neuronal survival, growth, development, and synaptic plasticity. Specifically, the downstream phospholipase Cγ (PLCγ) pathway in the BDNF/TrkB signaling cascade may lead to the activation of cAMP-response element binding protein (CREB) via calcium signaling, thereby influencing the expression of postsynaptic density protein 95 (PSD-95) and synaptophysin (Syn), both of which are crucial for neuronal synaptogenesis and plasticity[13]. Our study revealed that HPC may upregulate BDNF expression and activate BDNF/TrkB/PLCγ signaling, ultimately enhancing spatial cognition in mice[12]. Furthermore, individuals with depression exhibit disruptions in axonal branching, neurogenesis, synaptogenesis, and synaptic plasticity in the hippocampus, which are representative aspects of the pathophysiology of depression[14]. Thus, HPC may regulate BDNF levels and activate BDNF signaling, affecting neuronal survival, differentiation, and synaptic function to alleviate depression-like behaviors.

While BDNF may be a key target of HPC in depression treatment, the upstream regulators of BDNF signaling and other important molecules and their regulatory mechanisms in HPC neuroprotection are still unclear. Noncoding RNAs (ncRNAs), such as long noncoding RNAs (lncRNAs), circular RNAs (circRNAs), and microRNAs (miRNAs), have recently been implicated in the development of depression. These ncRNAs may act as diagnostic markers for depression[15] and regulate the expression of fundamental molecules related to depression, such as BDNF[16]. However, there is a lack of research on changes in the RNA transcriptome following HPC intervention in depression. Therefore, whole transcriptome sequencing is essential for identifying potential genes that are involved in the alleviation of depression by HPC and their regulatory mechanisms.

To investigate the aforementioned hypothesis, we established a 24-hour restraint stress mouse model to mimic depression-like behaviors and evaluate the impact of HPC on behaviors and biochemical markers. Following HPC treatment in the mouse model, we measured changes in BDNF and TrkB receptor expression; BDNF/TrkB signaling activation; and neuronal differentiation, development, and synaptic function. We subsequently employed whole transcriptome sequencing to identify RNAs and their regulatory networks involved in the above processes. This comprehensive approach aimed to elucidate the intricate molecular mechanisms through which HPC applies its antidepressant and endogenous neuroprotective effects and its effects on BDNF and BDNF signaling.

Materials and methods

Animals

SPF-grade ICR male mice, aged 6–8 weeks and weighing 18–22 g, were procured from SiPeiFu (Beijing) Biotechnology Co., Ltd. The mice were housed in a controlled environment with a temperature of 23 °C ± 3 °C and humidity ranging from 30 to 70%. Twenty animals per cage were provided with ad libitum access to food and water, under a 12-hour light-dark cycle. In addition, the body weights of the mice in each group were measured daily until the end of the behavioral tests. All methods were performed in accordance with the guidelines of National Institutes of Health and the Medical Ethics Review Committee of Baotou Medical College, and were approved by the Medical Ethics Review Committee of Baotou Medical College (approval numbers: 2021034. April 19, 2021). All experimental methods were conducted in accordance with the ARRIVE guidelines. All methods were carried out in accordance with relevant guidelines and regulations. After all behavioral tests were completed, mice were deeply anesthetized with sodium pentobarbital (Sigma-Aldrich, St Louis, MO, USA) and euthanized using cervical dislocation.

HPC treatment

HPC treatment was conducted following the protocol established in our previous study[12]. Briefly, a mouse was initially placed in a 125 ml jar filled with fresh air and sealed with a rubber stopper to create an airtight environment. Upon observing significant gasping breath in the mouse, it was promptly transferred to another 125 ml jar. This process was repeated four times to complete the HPC treatment. After 24 h of completing the HPC treatment, a subsequent 24-hour restraint stress was administered.

The 24-hour restraint stress

Mice were given 24-hour restraint stress as per protocol described by Chu et al.[17]. A mouse was confined in well-ventilated and transparent plastic tubes measuring approximately 3 cm in diameter and 10 cm in length. The mouse remained restrained in these tubes from 9:00 am to 9:00 am the next day. Throughout the restraint period, the mouse was placed in a dark environment with background noise coming from air-conditioning vents, and access to food and water was restricted. Small holes (approximately 0.5 cm in diameter) were strategically placed on the sides and head of the tubes to allow the mouse to defecate and dissipate heat. The mouse was permitted

to move its forelimbs and head, but hind limb movement was limited inside the tubes. Following the completion of the restraint, the mouse was immediately returned to cages with unrestricted access to food and water. Behavioral experiments were performed immediately after the end of restraint. Mice that were not subjected to restraint were kept in cages until just before the start of behavioral experiments.

Open field test (OFT)

OFT was firstly performed after the completion of restraint stress. The mice were placeded into a 50 cm×50 cm×50 cm open area and their initial positions were standardized to ensure consistency. They were allowed to explore for a period of 5 min. The movement trajectories of mice in OFT, including total distance, side distance, resting time, and exercise time, were recorded using OFT-100 experimental analysis system (Taimeng Software Co., Ltd., Chengdu, China). Prior to each test, the floor was cleaned with 75% alcohol to remove feces and urine, minimizing odors and cues.

Sucrose preference test (SPT)

SPT was subsequently exerted at 24 h intervals after the completion of OFT. Each mouse was housed individually in a cage with two drinking bottles containing distilled water and 2% sucrose solution respectively, along with food, for a 2 days habituation period. The position of the two bottles was alternated every 12 h to prevent the mice from developing memory of locations. On the first day of the official experiment, the mice were deprived of water and food for 24 h starting at 8 am. The diet was reinstated on the second day at the same time, and the mice were given bottles with distilled water and 2% sucrose solution, with the positions of the bottles changed every 12 h. Finally, the consumption of the 2% sucrose solution and distilled water by the mice was measured at 8 am on the third day.

Enzyme-linked immunosorbent assay (ELISA)

Following completion of all behavioral experiments, mice were anesthetized with sodium pentobarbital (Sigma-Aldrich, St Louis, MO, USA) and euthanized using cervical dislocation. The hippocampus was then extracted from the brain, weighed, and mixed with PBS at a ratio of 1:9 (g/mL). Subsequently, the hippocampus was homogenized then centrifuged at 4 °C and 8000 rpm for 10 min, with the resulting supernatant being collected. The levels of hippocampal neurotransmitters were assessed using corticosterone (CORT) and serotonin (5-HT) commercial ELISA kits (Jiangsu Jingmei Biotechnology Co., Ltd., Jiangsu, China) following the manufacturers's protocols. Additionally, the hippocampal oxidation index was determined through the use of malondialdehyde (MDA), superoxide dismutase (SOD), and catalase (CAT) ELISA kits (Sangon Biotech Co., Ltd., Shanghai, China).

Quantitative real-time PCR

The TRIzol reagent (Invitrogen, Carlsbad, CA, USA) was used to extract total RNA from mice hippocampus. After measurement of concentration, 1 μg of the extracted total RNA was reverse-transcribed into cDNA using RevertAid First Strand cDNA Synthesis Kit (Thermo Fisher Scientific Baltics UAB, Vilnius, Lithuania). Then, quantitative real-time PCR was execute to detect mRNA expression via SGExcel FastSYBR Mixture (Sangon Biotech Co., Ltd., Shanghai, China) using the following thermal cycling parameters: initial denaturation at 95°C for 10 min; subsequently 95°C for 30 s, 58°C for 30 s, and 72°C for 30 s with 40 cycles, final extension at 72°C for 2 min. Primer sequences were as follows: BDNF forward primer: 5′-tctgacgacgacatcactggc-3′, reverse primer: 5′-ccagcagaaagagtagaggaggc-3′. TrkB forward primer: 5′-gagctgctgaccaacctcca-3′, reverse primer: 5′-gtccccgtgcttcatgtactca-3′. β-actin forward primer: 5′-ggctgtattcccctccatcg-3′, reverse primer: 5′-ccagttggtaacaatgccatgt-3′. The experiments were conducted on an Applied Biosystems 7900 system (Applied Biosystems, Foster City, CA, USA) and relative expressions were calculated with $2^{-\Delta\Delta Ct}$ method.

Western blot

The mouse hippocampus was treated with RIPA buffer (Beyotime Institute of Biotechnology, Shanghai, China) and was sonicated to extract supernatant protein stock. Following determined of protein concentration using the BCA method (Livning Biotechnology Co., Ltd., Beijing, China), the proteins were separated on SDS-polyacrylamide gels and transferred to PVDF membranes (Roche, Mannheim, Germany). These membranes were then incubated overnight at 4 °C with the following primary antibodies: BDNF (1:1000, Abcam, MA, USA), TrkB (1:200, Santa Cruz, CA, USA), Phospho-TrkB Tyr816 (1:1000, Cell Signaling Technology, MA, USA), PLCγ1 (1:1000, Cell Signaling Technology, MA, USA), Phospho-PLCγ1 Tyr783 (1:1000, Cell Signaling Technology, MA, USA), CREB (1:1000, Cell Signaling Technology, MA, USA), Phospho-CREB Ser133 (1:1000, Cell Signaling Technology, MA, USA), PSD-95 (1:1000, Thermo Fisher, CA, USA), β-actin (1:1000, Santa Cruz, CA, USA). Subsequently, the PVDF membranes were incubated with a suitable HRP-coupled secondary antibody for 1 h at room temperature. Finally, the membranes were exposed using Super ECL Plus+ (Applygen, Beijing, China). Grey values were analysed using Image J, with β-actin serving as an internal reference to normalize the intensity of the bands.

Immunofluorescence staining

Mice were perfused with a 4% paraformaldehyde and saline under deep anesthesia. Then whole brains were collected and fixed in 4% paraformaldehyde at 4 °C overnight. The fixed brains underwent dehydration in 30% sucrose for 72 h. Following embedding in OTG, the brains were sectioned into 14 μm thick coronal cryosections using Cyrostar NX50 (Thermo Fisher Scientific, Waltham, MA, USA). These sections were then blocked with 10% goat serum (Boster, Wuhan, China) for 1 h at room temperature, followed by incubation overnight with BDNF primary antibody (1:500, Abcam, MA, USA), doublecortin (DCX) (1:500, Abcam, MA, USA), or neuronal

nuclei (NeuN) (1:500, Sigma-Aldrich, MO, USA) at 4 °C. Next, the sections were treated with Alexa Fluor Plus 488 goat anti-rat IgG secondary antibody (Invitrogen, Carlsbad, CA, USA) for 1 h at 4 °C in the absence of light and Hoechst (Beyotime Institute of Biotechnology, Shanghai, China) for 10 min at room temperature. Subsequently, images were captured using Nikon A1R + confocal microscopy system (Nikon, Melville, NY, USA) at 10X and 20X magnification and processed with NIS Elements C confocal-specific software (Nikon, Melville, NY, USA).

Golgi staining and Sholl analysis

The whole brains were collected from each group of mice and processed according to the manufacturer's protocol for the FD Rapid GolgiStain Kit (FD Neurotechnologies, MD, USA). The prepared brains were sectioned into 150 μm coronal cryosections using the Cyrostar NX50. Then sections were mounted on gelatin-coated slides, and Golgi staining was performed according to the kit instructions. The Eclipse Ci-L microscope (Nikon, Tokyo, Japan) was used to visualize and capture the stained pyramidal neurons in the hippocampus. Afterward, the total numbers of dendritic spines, as well as mushroom, thin and stubby spines, were quantified within the 30–90 μm length range of the 2nd or 3rd dendritic branch of the neuron using Image-Pro Plus 6.0 (Media Cybernetics, MD, USA). The number of dendritic spines per 10 μm was calculated as total numbers of spines/length of dendrites×10. The structure of the neuron was outlined using Image J, and the Sholl analysis was employed to generate 10 concentric circles with 10 μm spacing at the center of the neuron. The intersections of dendrites with these concentric circles were recorded, and the total sum of intersections across the 10 circles was calculated.

Whole transcriptome sequencing

Total RNA was extracted from the mouse hippocampus using TRIzol reagent, and the concentration was determined. RNA quality was assessed by a 5300 Bioanalyzer (Agilent, CA, USA). High-quality RNA samples were utilized for the construction of sequencing library (OD260/280 = 1.8–2.2, OD260/230 ≥ 2.0, RIN ≥ 6.5, 28 S:18 S ≥ 1.0, > 1 μg). The mRNA + lncRNA + circRNA libraries were prepared with the Illumina Stranded Total RNA Prep Ligation with Ribo-Zero Plus workflow (Illumina, CA, USA) according to the manufacturer's instructions. Additionally, a small RNA library was produced by the QIAseq miRNA Library Kit (Qiagen, Hilden, Germany). Then, whole transcriptome sequencing was conducted on an Illumina NovaSeq 6000 by Shanghai Majorbio Bio-pharm Biotechnology Co., Ltd. (Shanghai, China). Consequently, the clean data obtained were aligned with the reference genome to generate mapped data for further analysis such as transcript assembly, identification and prediction of novel RNAs, and expression calculation. Moreover, the quality of the sequencing results was evaluated focusing on saturation, gene coverage, distribution of reads in the reference genome and across different chromosomal regions, via HiSat2 (http://ccb.jhu.edu/software/hisat2/index.shtml) and Bowtie2 (http://bowtie-bio.sourceforge.net/bowtie2/index.shtml).

Differentially expressed RNA (DERNAs) identification

Following the acquisition of read counts, DESeq2 in R software was employed to estimate differentially expressed lncRNAs (DElncRNAs), circRNAs (DEcircRNAs), miRNAs (DEmiRNAs), and mRNAs (DEmRNAs) between different comparison groups. The screening criteria for significantly different DElncRNAs, DEcircRNAs and DEmRNAs were set as p-value < 0.05 and $|\log_2 FC| > 1$. And thresholds of Fold Change>1 and p-value < 0.05 were applied to identify significant DEmiRNAs.

Cluster analysis of DERNAs

Using the heatmap2 function from the R package, DElncRNAs, DEcircRNAs, DEmiRNAs, DEmRNAs were analyzed by clustering their FPKM values. These DERNAs exhibiting identical or similar expression patterns were grouped into classes, with each column representing an individual sample.

Establishment of CeRNA network

Target genes of miRNA and binding sites of lncRNAs and circRNAs to miRNAs were predicted using TargetScan and miRanda. The position of the lncRNA located on the upstream or downstream of mRNA, binding ability of the lncRNA to the mRNA, and the correlation between the lncRNA and mRNA expression, were considered in predicting potential targets of lncRNA. Based on the target genes, the number of microRNA response elements (MREs), and expression correlations between DERNAs, a competing endogenous RNAs (ceRNAs) network was constructed to explore the competitive binding of DElncRNAs, DEcircRNAs, DEmiRNAs and DEmRNAs, revealing a complex post-transcriptional regulatory network. This network included lncRNA-miRNA-mRNA pairs, circRNA-miRNA-mRNA pairs, visualized using Cytoscape.

GO and KEGG functional enrichment analysis of DERNAs

Target genes of DElncRNAs, DEcircRNAs and DEmiRNAs, as well as DEmRNA and ceRNA network were processed with the Gene Ontology (GO) term and Kyoto Encyclopedia of Genes and Genomes (KEGG) pathway functional enrichment analysis[18,19]. Goatools (https://github.com/tanghaibao/GOatools) was employed for GO analysis through Fisher's exact test. To control the false positive rate, four multiple tests (Bonferroni, Holm, Sidak, and False Discovery Rate) were applied to correct the p-value. A corrected p-value ≤ 0.05 indicated significant enrichment of the GO term. KOBAS (http://kobas.cbi.pku.edu.cn/home.do) was employed for KEGG analysis, following a similar principle as the GO analysis. A corrected p-value threshold of 0.05 was set, defining KEGG pathways with this value as significantly enriched in the DERNAs.

Statistical analysis

Experimental data were presented as mean ± SEM. Statistical comparisons among multiple groups were performed with analysis of variance (ANOVA), while comparisons between two groups were analyzed by t-test. Statistical significance was defined as $P < 0.05$.

Results

HPC alleviates depression-like behaviors in restraint stress model mice

At the beginning, we observed the changes in body weight across the groups. The control group exhibited a normal and stable increase in body weight, while the HPC group displayed a similar trend (Fig. 1a), indicating that HPC treatment alone did not induce body weight changes in mice. Following restraint stress, the weight of the mice significantly decreased, aligning with typical depressive symptoms (Fig. 1a, $P < 0.05$). Furthermore, at 0, 24 and 48 h post-restraint stress, the weight and weight gain in model mice remained lower than control group (Fig. 1a and b, $P < 0.05$). After HPC treatment followed by restraint stress, the weight of the mice also significantly decreased compared with the control group (Fig. 1a and b, $P < 0.05$), and was no notable changes post-restraint stress compared with the model mice (Fig. 1a and b, $P > 0.05$). The results might indicate that mice subjected to restraint stress demonstrate depressive-like weight loss, while HPC might not significantly affect the weight of the control and model mice.

Compared with the control group, the restraint stress model group presented decreased total distance (Fig. 1c, $P < 0.05$), side distance (Fig. 1d, $P < 0.05$) and exercise time (Fig. 1f, $P < 0.05$) and increased rest time (Fig. 1e, $P < 0.05$) in the OFT; furthermore, the model group presented reduced sucrose consumption in the SPT (Fig. 1g, $P < 0.05$). These typical depression-like behaviors confirmed the successful establishment of the model in mice through 24-hour restraint stress. After HPC treatment, the model mice illustrated increased total distance (Fig. 1c, $P < 0.05$), side distance (Fig. 1d, $P < 0.05$), and exercise time (Fig. 1f, $P < 0.05$) and decreased rest time (Fig. 1e, $P < 0.05$) in the OFT. HPC treatment also led to increased sucrose consumption (Fig. 1g, $P < 0.05$) in the model mice. These results suggest that HPC might ameliorate characteristic depression-like behaviors in restraint stress model mice.

HPC downregulates CORT and upregulates 5-HT in restraint stress model mice and enhances antioxidant capacity

Depression symptoms often coincide with the abnormal release of HPA axis-related hormones and neurotransmitters such as 5-HT, along with an imbalance in oxidative stress. Therefore, the levels of hormones and oxidative stress markers in the hippocampi of the mice were analyzed. Our findings revealed elevated levels of CORT (Fig. 2a, $P < 0.05$) and MDA (Fig. 2e, $P < 0.05$) in the restraint stress model group compared with the control group, whereas 5-HT, CAT, and SOD levels were decreased (Fig. 2b–d, $P < 0.05$), reflecting a typical

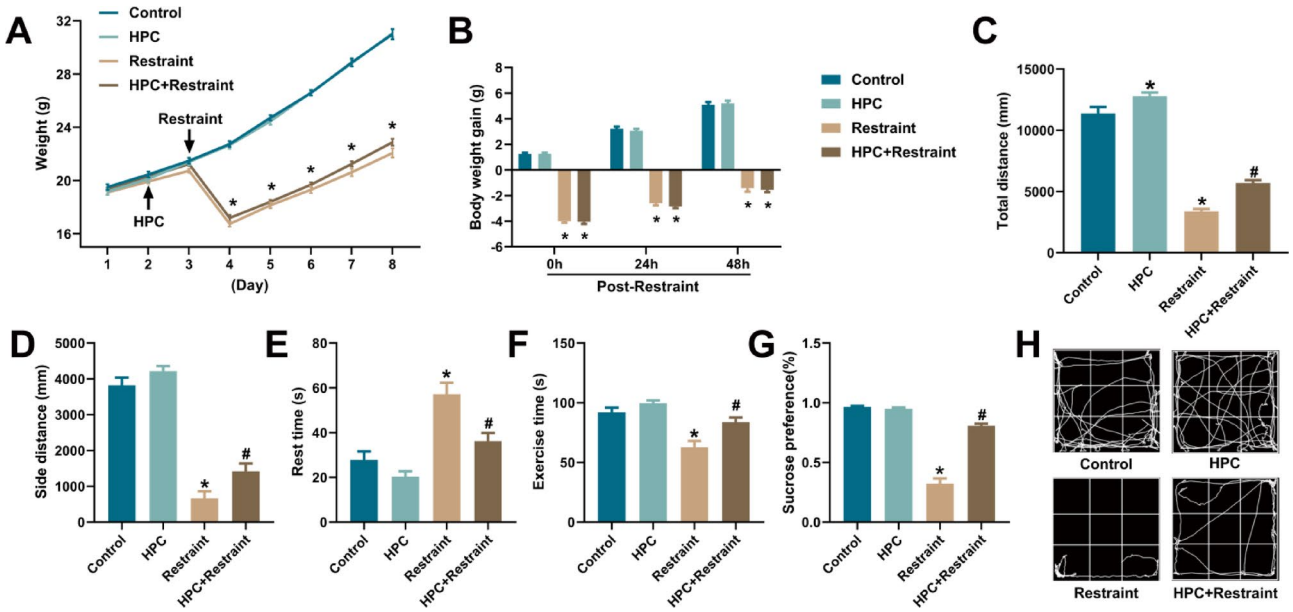

Fig. 1. HPC improves depression-like behaviors in restraint stress model mice. (**A**) The daily body weight of each group of mice during the experiment. (**B**) The body weight gain of each group (the body weight at 0, 24 and 48 h post-restraint stress minus the weight before restraint stress). Total distance (**C**), Side distance (**D**), Resting time (**E**), Exercise time (**F**) in the OFT. (**G**) Sucrose consumption of mice in the SPT. (**H**) Representative movement trajectories of each group of mice in the OFT. Data presented as mean ± SEM, $n = 20$ for body weight observation, $n = 12$ for OFT and SPT. * represents a statistically significant compared to the control group, with $P < 0.05$. # represents a statistically significant compared to the restraint stress model, with $P < 0.05$.

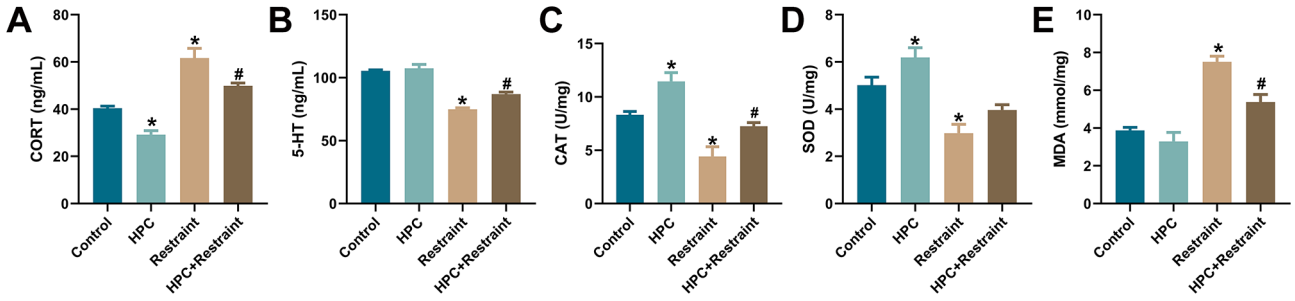

Fig. 2. HPC ameliorates hormones levels and oxidative stress in the hippocampus of restraint stress model mice. The levels of CORT (**A**), 5-HT (**B**), CAT (**C**), SOD (**D**), and MDA (**E**) in the hippocampus of mice. Data presented as mean ± SEM, $n = 6$. * represents a statistically significant compared to the control group, with $P < 0.05$. # represents a statistically significant compared to the restraint stress model, with $P < 0.05$.

depressive state. Conversely, HPC administration reduced the CORT (Fig. 2a, $P < 0.05$) and MDA (Fig. 2e, $P < 0.05$) levels while increasing the 5-HT and CAT (Fig. 2b, c, $P < 0.05$) levels in the restraint stress model mice. Additionally, HPC demonstrated neuroprotective and antidepressant potential by lowering the level of CORT and increasing the levels of CAT and SOD in the control group (Fig. 2a, c, d, $P < 0.05$). Overall, the above results indicate that HPC might restore the release of hormones and neurotransmitters in a restraint stress model and reinforce antioxidant activity.

HPC upregulates BDNF expression in restraint stress model mice but does not affect TrkB receptor expression

Downregulated BDNF expression is a known marker of depression. Similarly, both BDNF mRNA (Fig. 3a, $P < 0.05$) and protein (Fig. 3c, $P < 0.05$) expression were downregulated in the hippocampi of the restraint stress model mice. The findings from this and our previous studies consistently revealed that HPC might upregulate BDNF expression in the mouse hippocampus (Fig. 3a, c, $P < 0.05$). Notably, compared with the model mice, the restraint stress model mice treated with HPC presented significant upregulation of BDNF mRNA (Fig. 3a, $P < 0.05$) and protein (Fig. 3c, $P < 0.05$) expression. In addition, immunofluorescence analysis revealed that the fluorescence intensity of the BDNF protein, which is localized in the DG region of the mouse hippocampus, was attenuated in the restraint stress model but enhanced after HPC treatment (Fig. 3e, f, $P < 0.05$). These results suggest that the HPC might upregulate the expression of BDNF in the hippocampi of restraint stress model mice. However, there was no significant change in TrkB receptor (the specific receptor for BDNF) expression before and after HPC treatment in the restraint stress model mice (Fig. 3b, d, $P > 0.05$), indicating that the antidepressant effects of HPC primarily involve BDNF.

HPC activates BDNF/TrkB signaling and the downstream PLCγ pathway in restraint stress model mice

Following binding to the TrkB receptor, BDNF can activate BDNF signaling. Consequently, the expression of BDNF, which changed before and after HPC treatment in the restraint stress model mice, is likely to impact the activation of BDNF/TrkB signaling. To investigate this, we utilized western blot to assess the phosphorylation status of key molecules involved in BDNF/TrkB signaling and the downstream PLCγ pathway. In the restraint stress model, the protein expression of phosphorylated TrkB (p-TrkB), phosphorylated PLCγ (p-PLCγ), and phosphorylated CREB (p-CREB) was lower than that in the control group, as were the p-TrkB/total TrkB ratios (Fig. 4a, $P < 0.05$), p-PLCγ/total PLCγ ratios (Fig. 4b, $P < 0.05$), and p-CREB/total CREB ratios (Fig. 4c, $P < 0.05$). These findings indicate the inhibition of BDNF/TrkB/PLCγ signaling in the restraint stress model mice. In contrast, HPC upregulated the protein expression of p-TrkB, p-PLCγ, and p-CREB in the restraint stress model mice, as well as increased the ratios of p-TrkB/total TrkB (Fig. 4a, $P < 0.05$), p-PLCγ/total PLCγ (Fig. 4b, $P < 0.05$), and p-CREB/total CREB (Fig. 4c, $P < 0.05$). Furthermore, HPC also elevated the phosphorylation levels of these proteins in the control group, increasing the ratio of phosphorylated proteins to their respective total proteins (Fig. 4a–c). These results prove that HPC may reactivate the BDNF/TrkB/PLCγ signaling that was suppressed in the restraint stress model mice, thereby exerting antidepressant effects.

HPC rescues synaptic structural deficits in restraint stress model mice

The activation of BDNF/TrkB signaling can influence the structure and function of neuronal synapses and synaptic plasticity via the downstream PLCγ pathway. In the restraint stress model, HPC was found to regulate BDNF/TrkB/PLCγ signaling. PSD-95 expression in the hippocampi of the mice was subsequently measured, and Golgi staining and Sholl analysis were employed to evaluate the dendritic complexity and spine density of the hippocampal DG neurons in the mice (Fig. 5a). The results demonstrated that the hippocampal DG neurons in the restraint stress model mice had significantly fewer total spines and a lower proportions of stubby spines than did those in the control mice (Fig. 5b, $P < 0.05$), as well as a decreasing trend in the proportion of thin spines. However, there were no obvious differences in the proportion of mushroom spines (Fig. 5b, $P > 0.05$). Sholl analysis revealed a decrease in the number of dendritic intersections against equidistant Sholl spheres in the hippocampal DG neurons of model mice compared with those in the control group (Fig. 5c). These

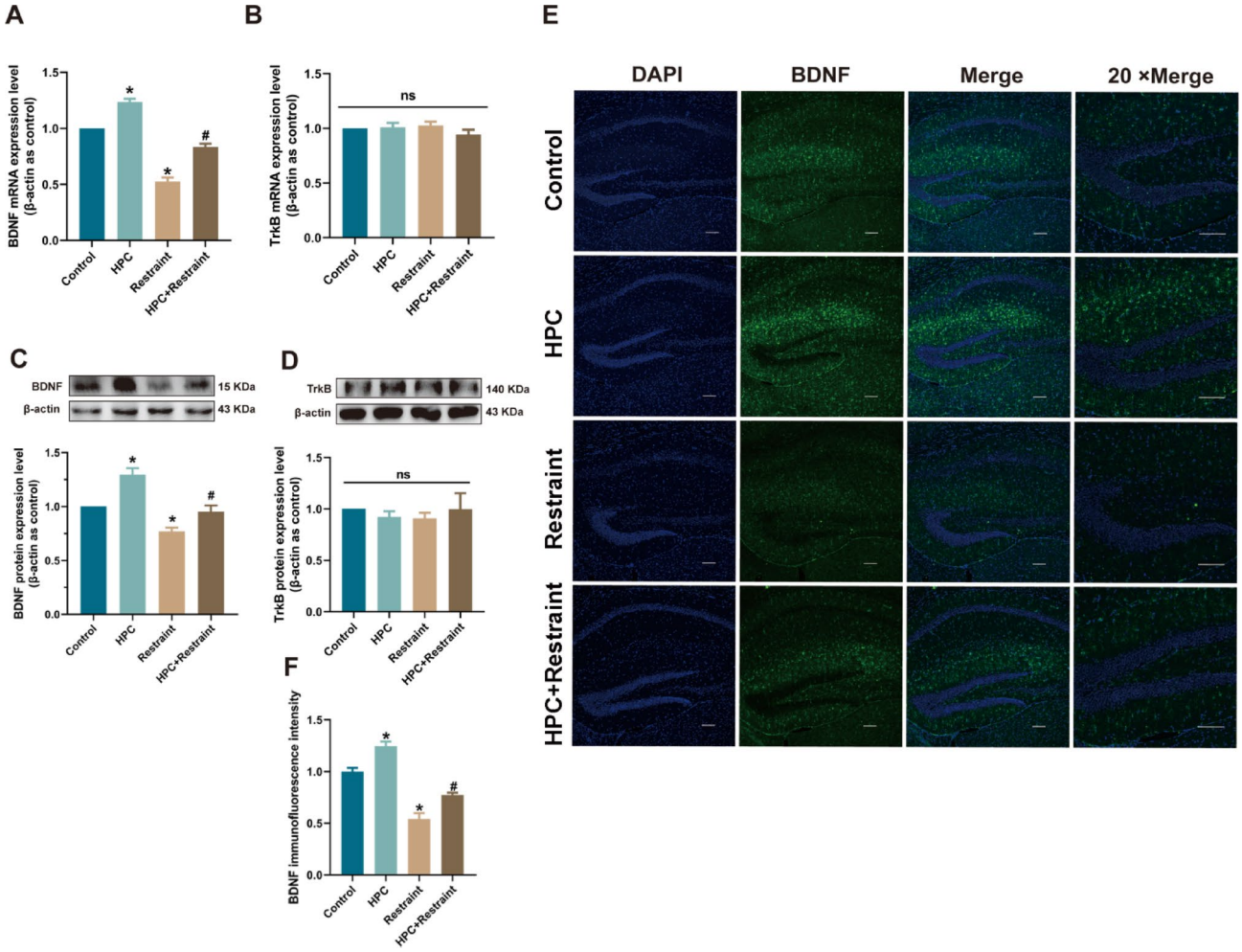

Fig. 3. HPC upregulates expression of BDNF in the hippocampus of restraint stress model mice. The qPCR was performed to detect the expression of BDNF (**A**) and TrkB receptor (**B**) at mRNA level in hippocampus of mice. The western blot was used to examine the expression of BDNF (**C**) and TrkB receptor (**D**) at protein level in hippocampus of mice. (**E**) Representative confocal images of BDNF immunofluorescence in the DG region of mouse hippocampus (20x), blue for DAPI, green for BDNF, Scale bars: 50 μm. (**F**) Immunofluorescence density values of BDNF. Data presented as mean ± SEM, $n = 6$ for qPCR and western blot, $n = 3$ for immunofluorescence. * represents a statistically significant compared to the control group, with $P < 0.05$. # represents a statistically significant compared to the restraint stress model, with $P < 0.05$.

data imply that dendritic atrophy occurred in the restraint stress model mice. Interestingly, HPC treatment resulted in increase in the total number of spines and the proportions of stubby and thin spines in the restraint stress model mice (Fig. 5b, $P < 0.05$), and there was no change in the proportion of mushroom spines (Fig. 5b, $P > 0.05$). Moreover, the reduction in the number of dendritic intersections in the restraint stress model was significantly abrogated by HPC (Fig. 5c). In addition, HPC upregulated the protein expression of PSD-95, which was downregulated in the mice subjected to restraint stress (Fig. 5d, $P < 0.05$). In summary, these findings suggest that the HPC might mitigate synaptic structural deficits in the restraint stress model mice by increasing the dendritic complexity and spine density of hippocampal DG neurons through the activation of BDNF/TrkB/PLCγ signaling, thus potentially improving symptoms of depression.

HPC promotes hippocampal neurogenesis in restraint stress model mice

Activated BDNF/TrkB signaling not only regulates the synaptic structure and function of neurons but also affects neuronal proliferation and neurogenesis. To examine the effects of the HPC on neurogenesis in the hippocampal DG region, we applied NeuN to label mature neurons and DCX to label newborn neurons. Our findings revealed that the immunofluorescence intensity of NeuN and DCX in the hippocampal DGs in the restraint stress model mice was notably lower than that in the hippocampal DGs in the control mice (Fig. 6a–d, $P < 0.05$), indicating a decrease in the number of newborn and mature neurons, consequently preventing hippocampal neurogenesis in the model. Following HPC treatment, the immunofluorescence intensity of NeuN and DCX in the hippocampal DGs of the restraint stress model mice increased (Fig. 6a–d, $P < 0.05$), indicating

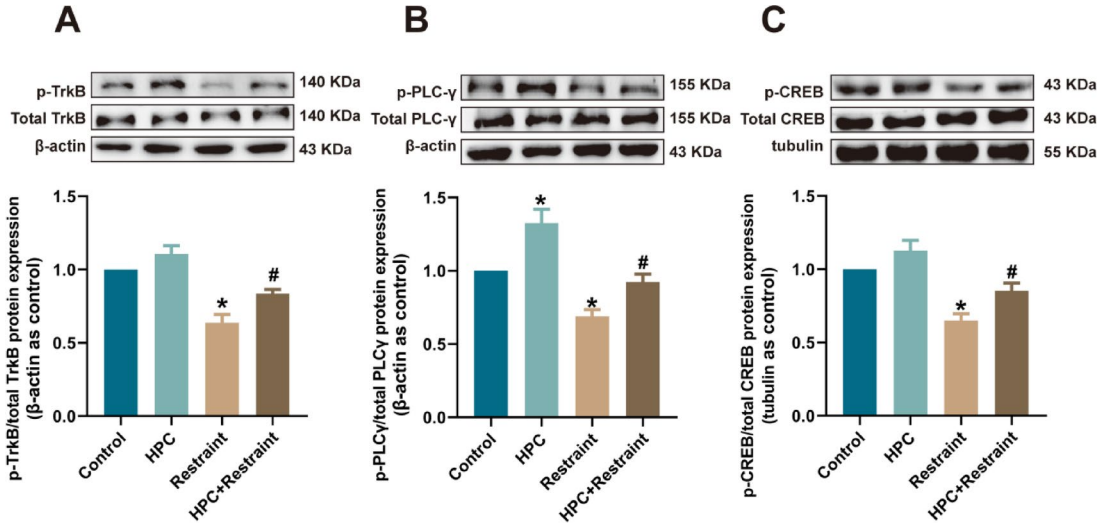

Fig. 4. HPC activates BDNF/TrkB/PLCγ signaling in the hippocampus of restraint stress model mice. The western blot analyzed phosphorylated and total proteins expression of TrkB (**A**), PLCγ (**B**), and CREB (**C**) in mouse hippocampus. Data presented as mean ± SEM, $n = 6$. * represents a statistically significant compared to the control group, with $P < 0.05$. # represents a statistically significant compared to the restraint stress model, with $P < 0.05$.

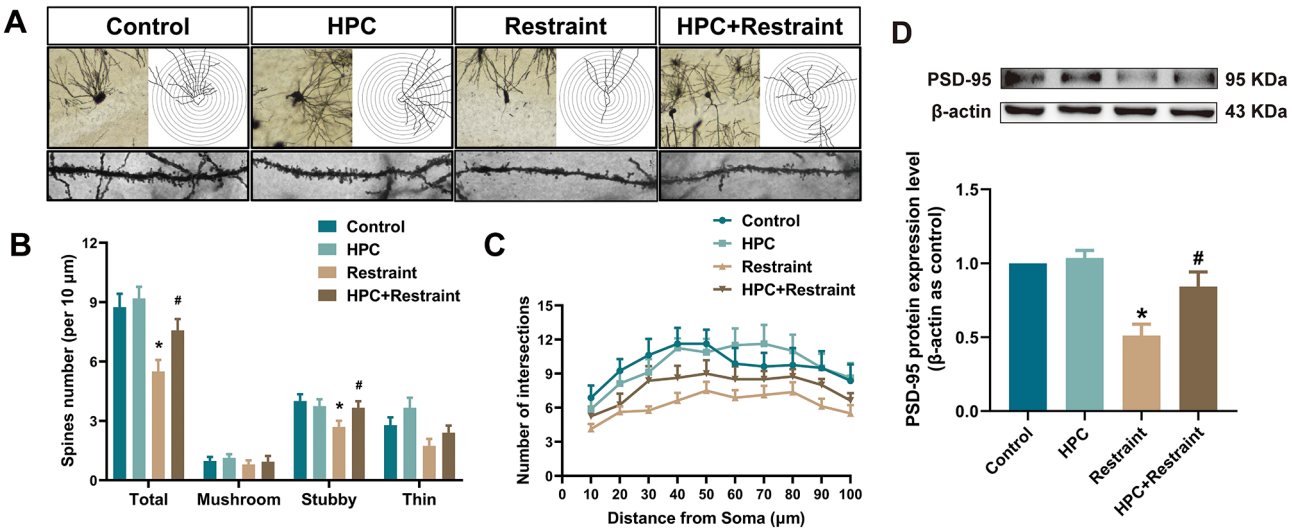

Fig. 5. HPC remedies dendritic complexity and spine density of hippocampal DG neurons in restraint stress model mice. (**A**) Representative images of Golgi staining and traces of Sholl analysis for hippocampal DG neurons and their dendritic spines. (**B**) The density of total spine and mushroom, stubby, thin spines in hippocampal DG neurons of mice. (**C**) The number of dendritic intersections for Sholl analysis in hippocampal DG neurons of mice. (**D**) The western blot detected protein expression of PSD-95 in mouse hippocampus. Data presented as mean ± SEM, $n = 8$ for Golgi staining, $n = 6$ for western blot. * represents a statistically significant compared to the control group, with $P < 0.05$. # represents a statistically significant compared to the restraint stress model, with $P < 0.05$.

increases in the numbers of newborn and mature neurons. These results propose that HPC has a protective effect on hippocampal neurogenesis in restraint stress model mice by activating BDNF/TrkB signaling.

Expression profiling and differential RNA expression analysis of restraint stress model mice before and after treatment with HPC using whole transcriptome sequencing

The experimental results demonstrated that HPC effectively alleviated depression-like behaviors by mediating neuronal synaptic structures and neurogenesis via BDNF signaling. To elucidate the upstream regulatory mechanisms of BDNF signaling during HPC resistance to depression, as well as to identify other potential molecules involved in the antidepressant effects of HPC through their influence on synapsis or neurogenesis,

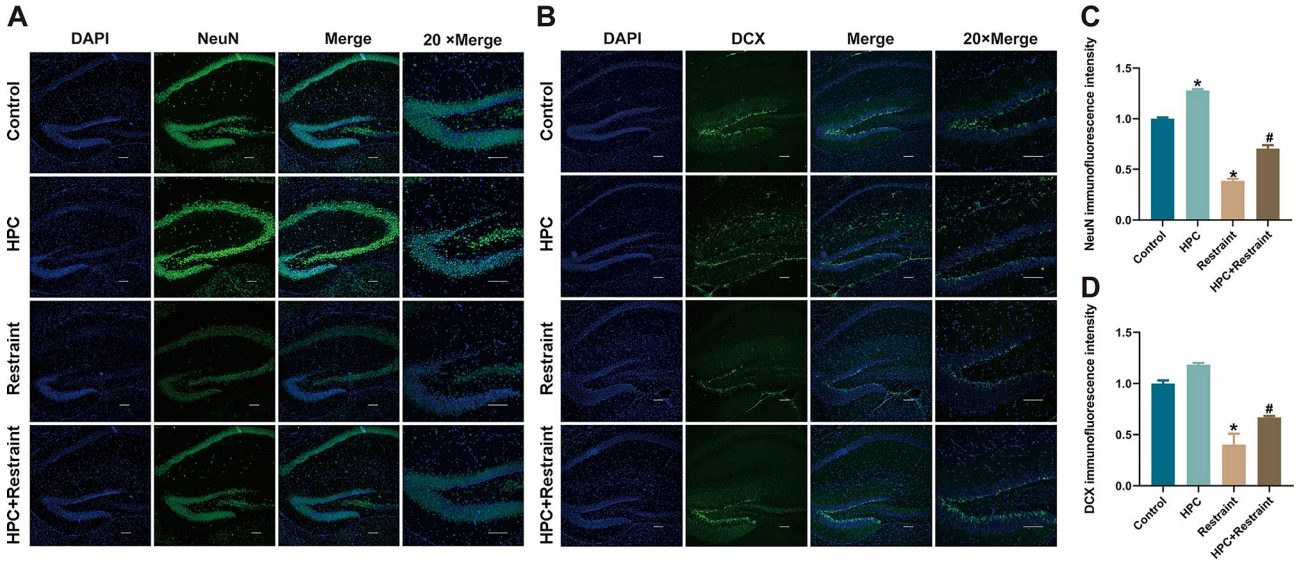

Fig. 6. HPC promotes hippocampal neurogenesis in restraint stress model mice. Representative confocal images of NeuN (**A**) and DCX (**B**) immunofluorescence in the DG region of mouse hippocampus (20x), blue for DAPI, green for NeuN and DCX, Scale bars: 50 μm. Immunofluorescence density values of NeuN (**C**) and DCX (**D**). Data presented as mean ± SEM, $n = 3$. * represents a statistically significant compared to the control group, with $P < 0.05$. # represents a statistically significant compared to the restraint stress model, with $P < 0.05$.

we employed whole transcriptome sequencing to analyze RNA expression in both restraint stress model mice and model mice treated with HPC. Initially, the distributions of different types of RNA across the above two groups were examined, with violin plots indicating an even distribution of lncRNA (Fig. 7a), circRNA (Fig. 7d), miRNA (Fig. 7g) and mRNA (Fig. 7j) in model mice and model mice treated with HPC. Furthermore, Venn diagrams revealed that 1755 lncRNAs (Fig. 7b), 451 circRNAs (Fig. 7e), 837 miRNAs (Fig. 7h) and 18,618 mRNAs (Fig. 7k) were concurrently expressed in the two groups, with the majority of the ncRNAs and mRNAs coexpressed. Notably, on the basis of the sequencing results and subsequent data analysis, we identified a total of 373 differentially expressed lncRNAs (DElncRNAs) in the HPC treated model group compared with the restraint stress model group, comprising 174 upregulated and 199 downregulated DElncRNAs. Additionally, 166 differentially expressed circRNAs (DEcircRNAs) were detected, 83 of which were upregulated and 83 downregulated. Furthermore, we discovered 29 differentially expressed miRNAs (DEmiRNAs), including 14 upregulated and 15 downregulated DEmiRNAs. Finally, 1235 differentially expressed mRNAs (DEmRNAs) were identified, consisting of 619 upregulated and 616 downregulated DEmRNAs. The volcano plots provide a comprehensive overview of the overall distribution of these differentially expressed RNAs (DERNAs) (Fig. 7c, f, i, l).

Cluster analysis of differentially expressed RNAs in restraint stress model mice before and after HPC treatment

Subsequently, the DERNAs between the restraint stress model mice and HPC treated model mice were subjected to clustering analysis. A heatmap was used to visualize significant differences in the characteristics of the DERNAs. The analysis revealed distinct lncRNAs (Fig. 8a), circRNAs (Fig. 8b), miRNAs (Fig. 8c), and mRNAs (Fig. 8d) between the two groups. Notably, the results of the clustering analysis were consistent with those obtained from the differential RNA expression analysis.

Functional enrichment analysis of differentially expressed RNAs in restraint stress model mice before and after HPC treatment

To illuminate the biological processes of DERNAs between restraint stress model mice and HPC treated model mice, we conducted Gene Ontology (GO) enrichment analyses on target genes of lncRNAs, circRNAs, and miRNAs, as well as mRNAs. The top 20 significantly enriched biological processes are shown in bubble diagrams on the basis of the enrichment factor (Fig. 9). Presynapse, regulation of transport, protein domain-specific binding, transcription coregulator binding, synapse and so on were enriched primarily in the DElncRNAs (Fig. 9a); whereas protein binding, glutamatergic synapses, neuronal cell bodies, regulation of axonogenesis, and nervous system development were significantly enriched in the DEcircRNAs (Fig. 9b); The DEmiRNAs were associated predominantly with cell morphogenesis, positive regulation of neurogenesis, regulation of synaptic plasticity, and regulation of dendrite development (Fig. 9c); The DEmRNAs were associated mainly with glutamatergic synapses, axons, regulation of transmembrane transport, the postsynaptic actin cytoskeleton, and dense bodies (Fig. 9d).

Kyoto Encyclopedia of Genes and Genomes (KEGG) pathway enrichment analyses were performed to further explore the functions of the DERNAs between the two groups. We focused on the top 10 or 20 significantly

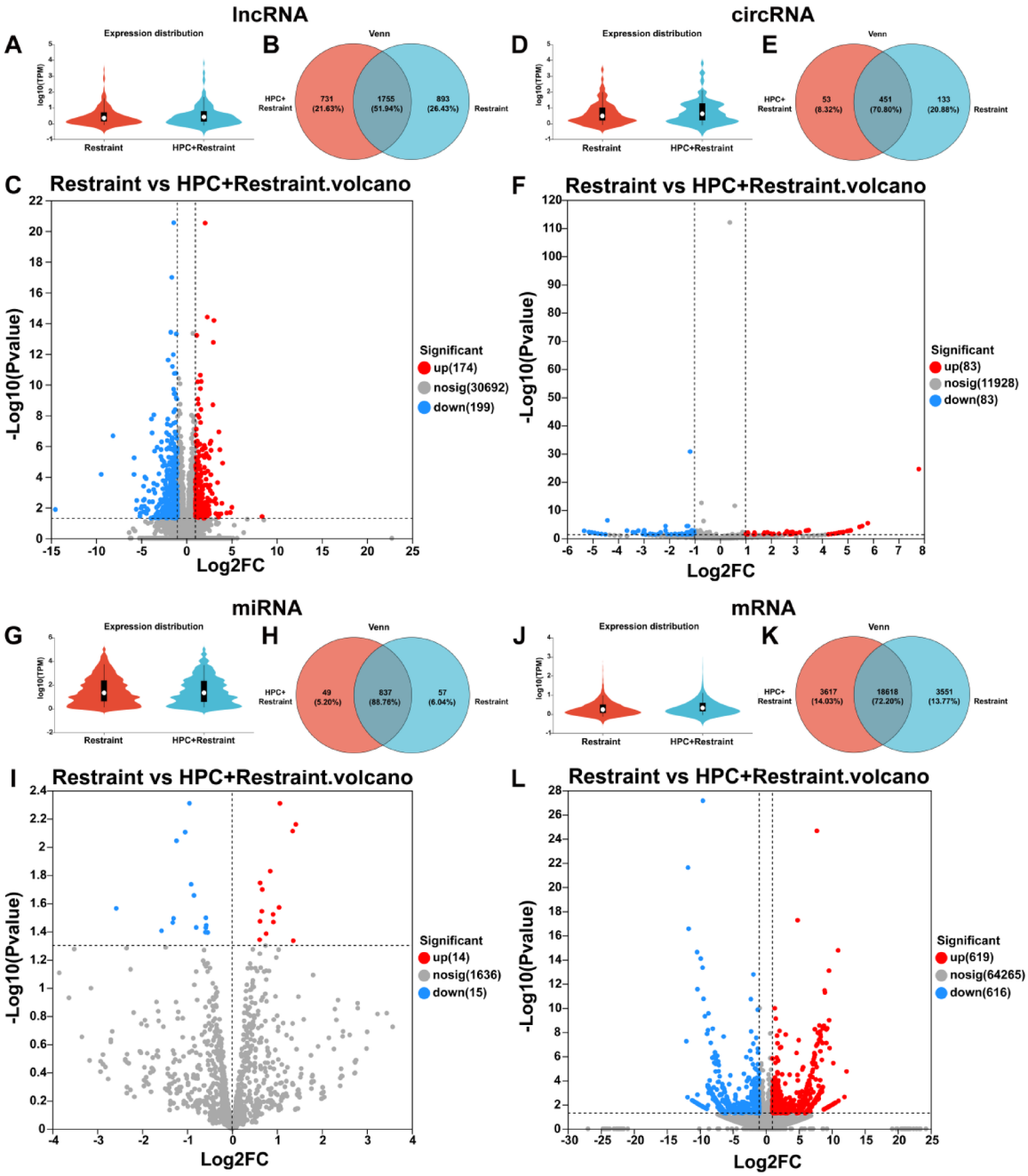

Fig. 7. Expression profiling and differential RNA expression analysis by whole transcriptome sequencing. Violin plots showing expression distribution of lncRNAs (**A**), circRNAs (**D**), miRNAs (**G**) and mRNAs (**J**) between restraint stress model mice and model mice treated with HPC. Venn plots showing co-expression of lncRNAs (**B**), circRNAs (**E**), miRNAs (**H**) and mRNAs (**K**). Volcano plots showing DElncRNAs (**C**), DEcircRNAs (**F**), DEmiRNAs (**I**) and DEmRNAs (**L**).

enriched pathways on the basis of the enrichment factor. Among these, the DElncRNAs were associated mainly with axon guidance, the MAPK signaling pathway, GABAergic synapse, the Phosphatidylinositol signaling system and other pathways (Fig. 9e); the DEcircRNAs were associated predominantly with axon guidance, GABAergic synapse, glutamatergic synapse, the MAPK signaling pathway, and the Phosphatidylinositol signaling system (Fig. 9f); the DEmiRNAs were significantly associated with axon guidance and regeneration, endocytosis, the Phosphatidylinositol signaling system, the neurotrophin signaling pathway, and the autophagy-animal pathway (Fig. 9g); and the DEmRNAs were associated primarily with tight junction, the neurotrophin signaling pathway, the regulation of actin cytoskeleton, the calcium signaling pathway, and the Ras signaling pathway (Fig. 9h).

These findings indicated that the GO terms associated with DElncRNAs, DEcircRNAs, DEmiRNAs, and DEmRNAs were linked to the regulation of synapses, axons and neurogenesis. Furthermore, the enriched KEGG pathways were related to synapses, axons, neurotrophin signaling and pathways downstream of the BDNF

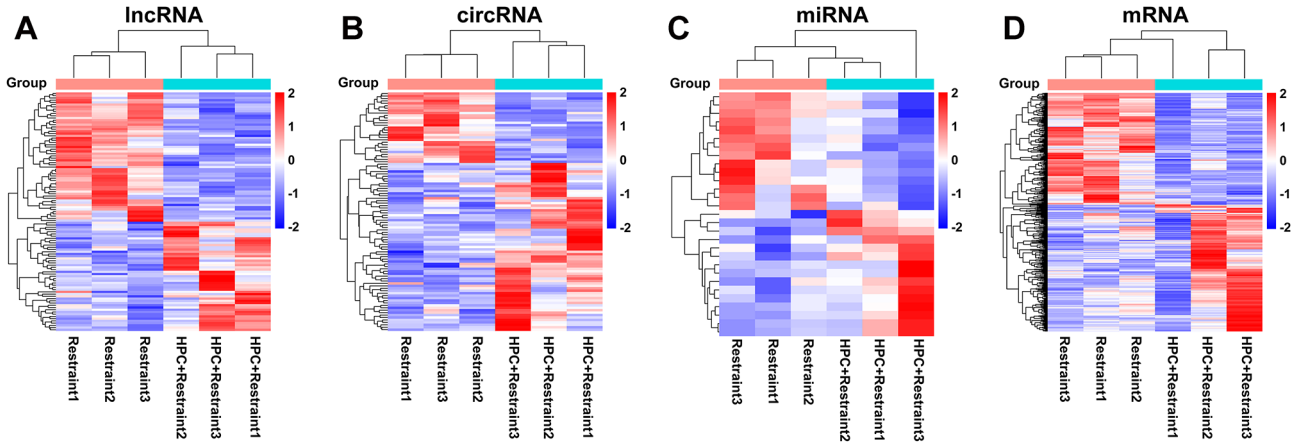

Fig. 8. Cluster analysis of differentially expressed RNAs. Heatmap plots DElncRNAs (**A**), DEcircRNAs (**B**), DEmiRNAs (**C**) and DEmRNAs (**D**) between restraint stress model mice and model mice treated with HPC. Red represents upregulated DERNAs, blue represents downregulated DERNAs.

signaling cascade. Therefore, it is reasonable to conclude that HPC may alleviate depression-like behaviors by influencing neuronal synaptic structure and function, as well as neurogenesis, under the coregulation of ncRNAs and BDNF signaling.

Construction of CeRNA networks for differentially expressed RNAs

Owing to the competitive adsorption of lncRNAs and circRNAs, which can lead to the inhibition of miRNA activity and the formation of competing endogenous RNAs (ceRNAs), these molecules may contribute to the antidepressant effects of HPC by regulating the expression of target genes. First, the 29 DEmiRNAs were subjected to three independent computational algorithms: TargetScan (for conserved targeting prediction), RNAhybrid (with filtering criteria: number of hits per target ≥ 100, binding energy≤-20 kcal/mol, and $P < 0.05$), and miRanda (using score threshold ≥ 160 and energy constraint≤-20 kcal/mol) to identify putative miRNA-mRNA interaction pairs. This integrative analysis yielded 239 target mRNA transcripts (Fig. 10a). Consequently, the DElncRNAs and DEcircRNAs were analyzed using the miRanda database (with score threshold ≥ 160 and energy threshold≤-20 kcal/mol) to predict miRNA response elements. After removing non-differentially expressed miRNAs, we constructed regulatory networks for lncRNA-miRNA-mRNA and circRNA-miRNA-mRNA guided by the ceRNA theory. These networks might interpret the regulatory relationships between ncRNAs and mRNAs. The lncRNA-miRNA-mRNA network comprised 26 lncRNAs, 17 miRNAs and 171 mRNAs, with 212 intersections identified (Fig. 10b). Moreover, the circRNA-miRNA-mRNA network consists of 10 circRNAs, 8 miRNAs, and 70 mRNAs, also featuring 89 intersections (Fig. 10c).

Functional enrichment analysis of the CeRNA networks

To further clarify the functions of the ceRNA networks, we administered GO and KEGG enrichment analyses on the DElncRNAs, DEcircRNAs, DEmiRNAs and DEmRNAs involved in the ceRNA networks. The results indicated that the GO terms related to positive regulation of biological and cellular processes, intracellular anatomical structure, postsynaptic density and specialization, neuron-to-neuron synapses, neurogenesis, glutamatergic and asymmetric synapses, and nervous system development were significantly enriched in the ceRNA networks (Fig. 11a).

KEGG enrichment analysis revealed that the ceRNA network was significantly associated with BDNF signaling and its downstream pathways, including the neurotrophin signaling, cAMP, mTOR and MAPK pathways (Fig. 11b). These findings suggest that DElncRNAs and DEcircRNAs within the ceRNA network mediate DEmiRNAs that likely regulate the expression of key molecules involved in BDNF signaling, synapses and neurogenesis, thereby contributing to the neuroprotective effects of HPC in ameliorating depression-like behaviors.

In brief, the experimental studies and whole transcriptome sequencing results collectively demonstrated that HPC might alleviate depression-like behaviors by mediating neuronal synaptic structure and function, as well as neurogenesis via BDNF signaling. Furthermore, this process might require lncRNAs, circRNAs, and miRNAs, particularly the ceRNA networks consisting of these RNAs, and several other important molecules associated with HPC and depression.

Discussion

The model developed in our study demonstrated the typical behavioral, physiological, and molecular changes associated with depression in mice following 24 h of restraint stress, which aligns with the results of the initial study of this model[17]. According to the stress hypothesis, prolonged periods of high stress, caused by factors such as hypoxia, may contribute to the onset of depression[20]. However, HPC actively triggers endogenous protective mechanisms to boost tissue and cell adaptation to hypoxia, offering notable protective effects on

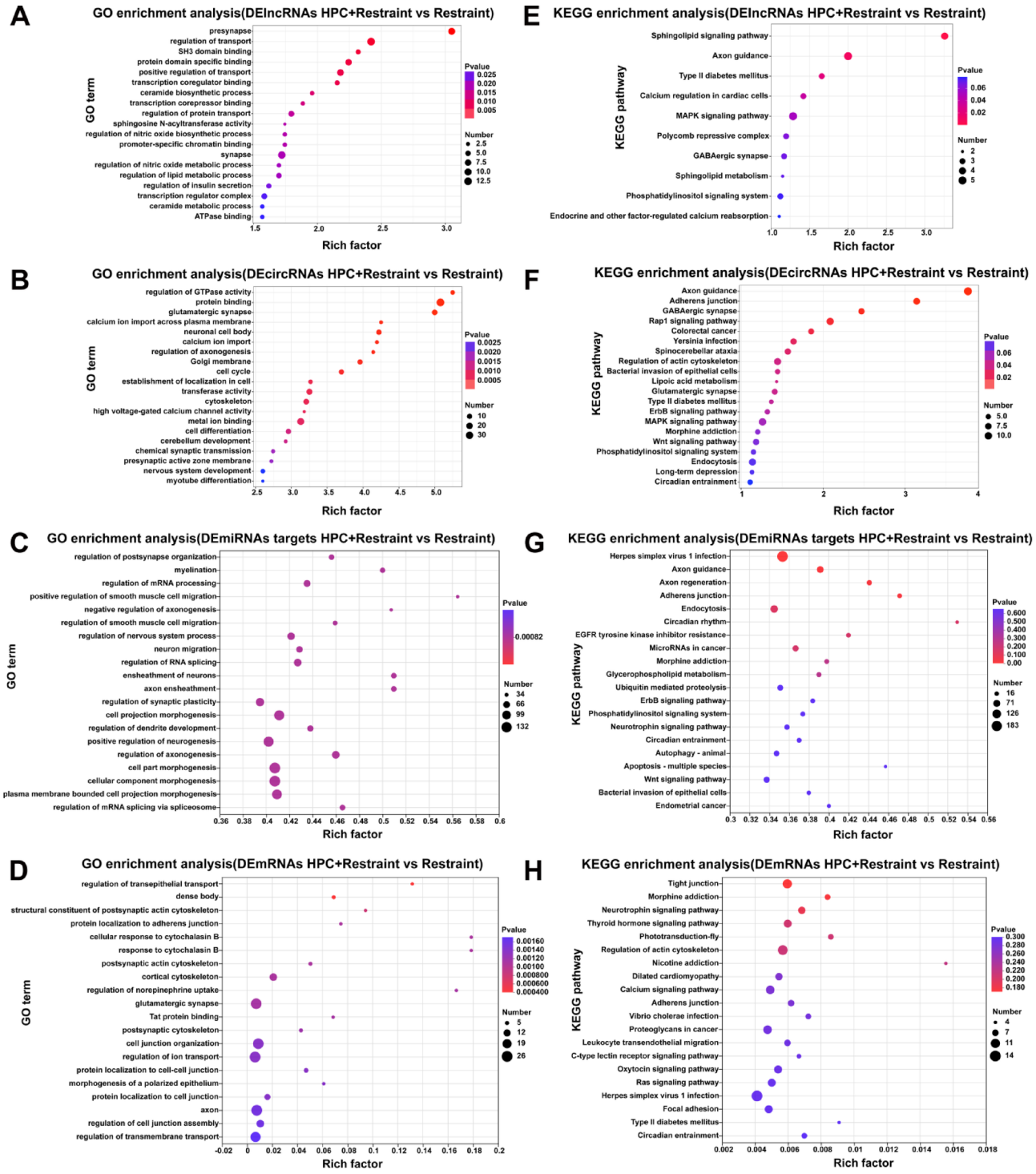

Fig. 9. Functional enrichment analysis of differentially expressed RNAs. GO functional enrichment analysis for DElncRNAs (**A**), DEcircRNAs (**B**), DEmiRNAs (**C**) and DEmRNAs (**D**) between restraint stress model mice and model mice treated with HPC. KEGG pathway functional enrichment analysis for DElncRNAs (**E**), DEcircRNAs (**F**), DEmiRNAs (**G**) and DEmRNAs (**H**).

the nervous system by alleviating oxidative stress, regulating hypoxia-inducible factor (HIF) expression, and promoting neurogenesis[5,21]. These mechanisms intersect with the underlying causes of depression, suggesting the potential of HPC to ameliorate depressive behaviors by counteracting the neurobiological alterations linked to depression progression. Previous studies have displayed that HPC might mitigate depression-like behaviors in a rat LH model involving the HPA axis, neuropeptides, and transcription factors[7,8,22]. Clinical investigations have also revealed that remote ischemic preconditioning (RIPC) effectively relieves symptoms

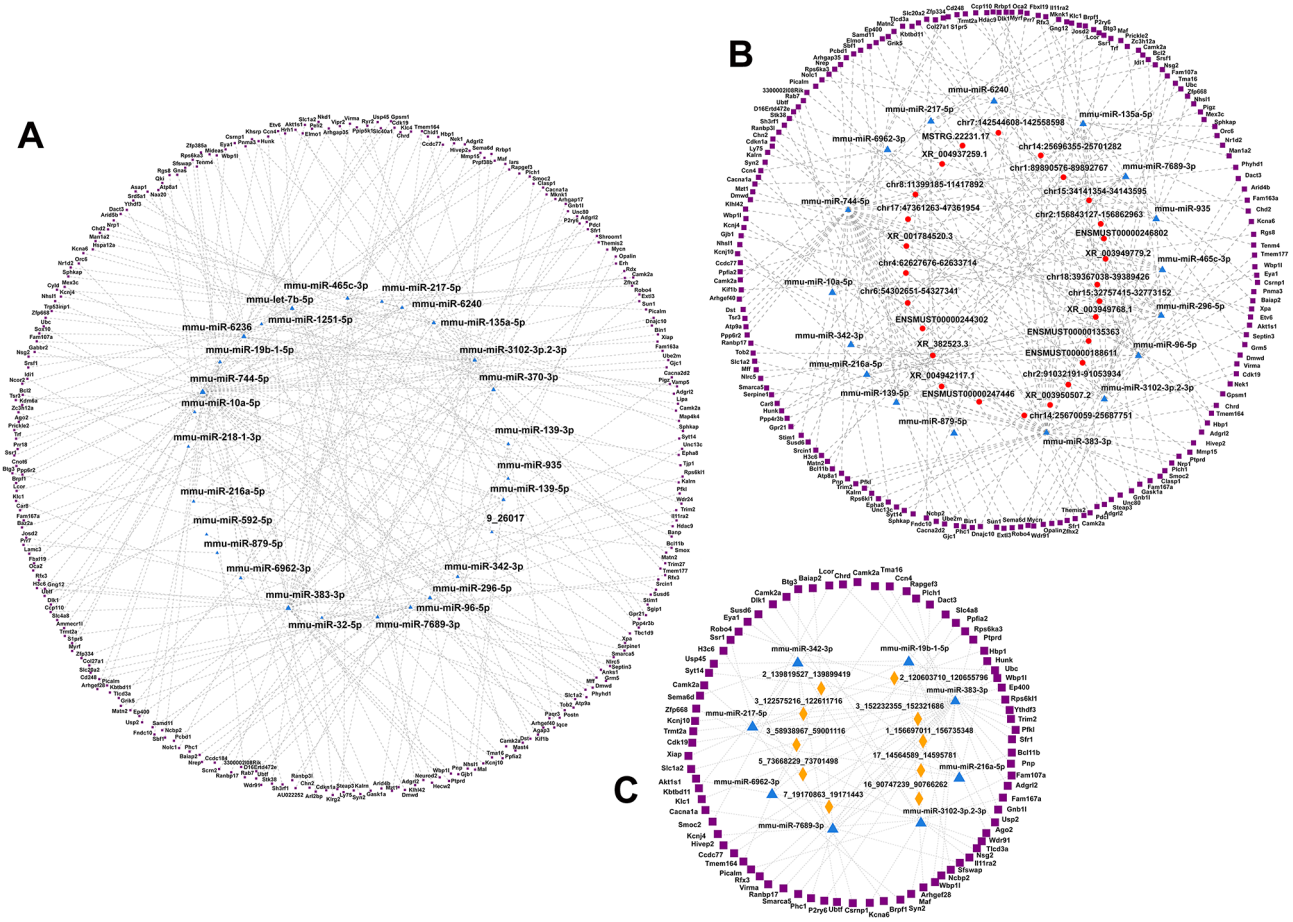

Fig. 10. The ceRNA networks of differentially expressed RNAs. (**A**) The miRNA-mRNA interaction network. (**B**) The ceRNA network of lncRNA-miRNA-mRNA. (**C**) The ceRNA network of circRNA-miRNA-mRNA. Red circle represents lncRNA, yellow rhombus represents circRNA, blue triangle represents miRNA, and purple square represents mRNA.

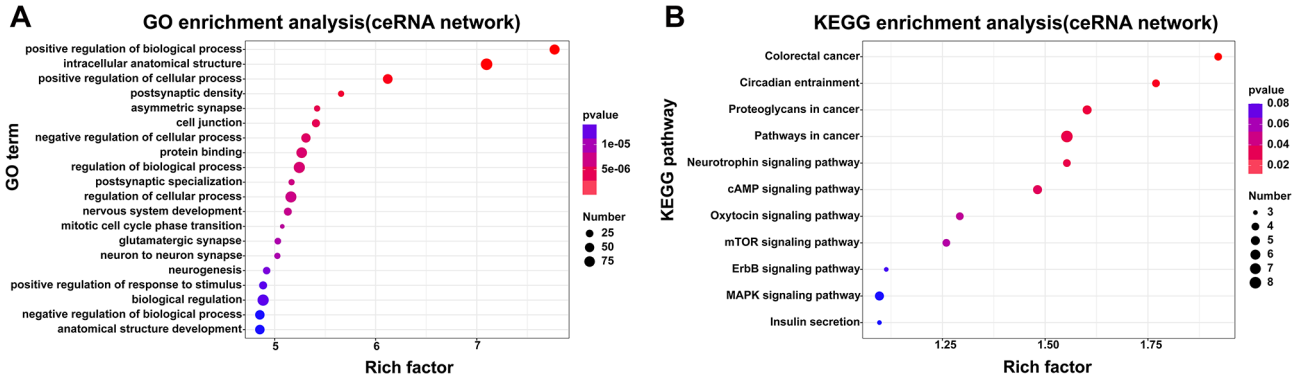

Fig. 11. Functional enrichment analysis for the ceRNA networks of RNAs. (**A**) GO functional enrichment analysis for the ceRNA networks of RNAs. (**B**) KEGG pathway functional enrichment analysis for the ceRNA networks of RNAs.

in MDD patients, with good safety and tolerance profiles[9]. Like HPC, certain hypoxia-related phenomena such as intermittent hypobaric hypoxia, also have neuroprotective effects on depression induced by chronic mild stress[23]. Furthermore, our findings indicate that HPC might prevent depression by influencing depression-like behaviors, hormone and neurotransmitter release, BDNF expression and signaling, synaptic structure and function, as well as hippocampal neurogenesis.

Our results showed that 24 h restraint stress might lead to weight loss in mice, a classic phenotype of depression. Although HPC might not generate a significant change in the weight of the model mice, a slight increasing trend was noted (Fig. 1a and b). This might be attributed to the short duration of body weight observation and the small sample size. Additionally, HPC has the potential to modulate brain metabolism[24,25], which might influence body weight through the gut-brain axis. The 6–8 weeks ICR mice we chose, might still be in a period of weight gain during the gradual maturation phase. Furthermore, exercise training[26], high-frequency repetitive transcranial magnetic stimulation[27], and other endogenous/non-invasive methods similar to HPC may also increase body weight while alleviating depressive behavior. In light of the aforementioned limitations and hypotheses, our future research will aim to further elucidate the impact of HPC on weight during the process of mitigating depressive-like behavior.

Chronic and mild stress stimuli can elevate the levels of antioxidant enzymes, such as SOD and CAT, which function to eliminate free radicals. However, with the occurrence of depressive-like behaviors, these enzymes may be gradually exhausted following stress induction over several weeks. Although our study did not immediately detect changes in SOD and CAT levels, including potential transient elevations at the termination of 24 h of restraint stress, we identified a rapid decline in SOD and CAT levels approximately one week post-restraint stress (Fig. 2c and d). Unlike chronic and mild stress, the 24 h restraint stress might trigger an explosive surge of free radicals within a short timeframe. While this acute stress might transiently upregulate antioxidant enzymes, the overwhelming oxidative burden could lead to accelerated depletion of SOD and CAT, resulting in the reductions of these enzymes one week post-restraint stress. HPC might reinforce the antioxidant activity of model mice by either facilitating an earlier release of SOD and CAT or slowing their depletion during restraint stress. Moreover, studies investigating acute restraint stress induced depressive-like behaviors have consistently reported reduced levels of antioxidant enzymes[28,29]. Indeed, systematic daily monitoring of oxidative stress markers throughout the experimental timeline should be required, and this has been incorporated into our subsequent experiments mentioned above.

Previous studies have highlighted the antidepressant effects of HPC, but the impact of BDNF on molecular mechanisms has been underexplored. BDNF serves as a crucial biomarker for depression onset, with decreased expression observed in depressed patients' serum and hippocampi postmortem[22,30]. Dysregulation of BDNF leads to atrophy, synaptic disconnection, and dysfunction in depression-related brain circuits. Conversely, optimizing BDNF levels increases expression of plasticity genes and neuronal function recovery, alleviating depressive symptoms. Interventions such as SSRIs or direct BDNF injection into the hippocampus may induce antidepressant effects[31,32]. In our extensive HPC research, we identified a potential mechanism in which 'bad genes' associated with brain damage are downregulated and 'good genes' with protective effects are upregulated under extreme conditions such as hypoxia[5,21,24]. BDNF, a prototypical 'good gene', is upregulated by HPC in the hippocampus, enhancing spatial cognitive abilities in mice[12]. These findings prompted us to investigate the antidepressant potential of HPC in a mouse depression model. As anticipated, HPC upregulated BDNF expression in the restraint stress model mice (Fig. 3), thereby improving depression-like behaviors (Figs. 1 and 2). Furthermore, intermittent hypoxia akin to HPC also elevates BDNF expression in the hippocampus, offering neuroprotective benefits in a rat depression model[23].

BDNF binds to TrkB receptors, activating BDNF/TrkB signaling, which affects neuronal survival via the phosphoinositide 3-kinase (PI3-K)/Akt pathway[33], regulates synaptic plasticity through the PLCγ pathway[34], and contributes to neural growth and differentiation through the mitogen-activated protein kinase (MAPK) pathway[35]. Reduced BDNF expression in depression may hinder the activation of BDNF/TrkB signaling, resulting in increased neuronal apoptosis, deficits in synaptic structure, and impaired neurogenesis and neural differentiation. Various interventions for depression that upregulate BDNF expression have been shown to abrogate these effects by reinvigorating BDNF/TrkB signaling[36,37]. Our previous studies demonstrated that HPC may mitigate neuronal apoptosis and promote neuroregeneration[38,39]. In particular, HPC upregulates BDNF and activates BDNF/TrkB/PLCγ signaling, which improves learning and memory in mice via the possible modulation of synaptic plasticity[12]. Therefore, the results of this study are not surprising because HPC might redeem synaptic structural deficits and promote hippocampal neurogenesis in restraint stress model mice. We speculate that HPC may upregulate BDNF in restraint stress model mice (Fig. 3), leading to activation of the BDNF/TrkB/PLCγ pathway (Fig. 4). PLCγ then generates inositol-1,4,5-trisphosphate (Ins(1,4,5)P3) and diacylglycerol (DAG), triggering the release of Ca^{2+} from intracellular stores and activating Ca^{2+}/CaM-dependent protein kinases (CaMK), such as CaMKII, CaMKK, and CaMKIV. Subsequently, CaMK initiates CREB, a transcription factor that modulates the expression of synaptic proteins such as PSD-95, ultimately modifying the synaptic structure in the model (Fig. 5). While our study confirmed the promotion of hippocampal neurogenesis in the restraint stress model mice following HPC treatment (Fig. 6), we did not observe the involvement of MAPK signaling in regulating this process. Therefore, our future research will focus on investigating the effects of HPC on MAPK signaling and the PI3-K/Akt signaling pathways responsible for neuronal survival. This will allow us to gain a more comprehensive understanding of the mechanisms through which HPC prevents the behavioral and pathophysiological aspects of depression.

Research has shown the significant role of BDNF and its signaling in HPC mediated alleviation of depression-like behaviors in mice. However, depression is a complex and heterogeneous condition influenced by multiple genes and molecular pathways. Consequently, additional critical factors may contribute to the antidepressant effect of HPC. Moreover, existing studies indicate that ncRNAs play essential regulatory roles in gene expression related to the neuroprotective effects of HPC[40] and the pathophysiology of depression[7]. Therefore, we employed whole transcriptome sequencing to elucidate the intricate molecular mechanisms involved. Our analysis revealed 373 DElncRNAs, 166 DEcircRNAs, 29 DEmiRNAs, and 1235 DEmRNAs in the hippocampus before and after the restraint stress model was established in HPC (Fig. 7). Among these DEmRNAs, in addition to BDNF, we also identified solute carrier (SLC) transporter family genes, excitatory amino acid receptors such

as Grm5 and Hrh1, Kalirin, Bcl2, Picalm, Pde10a, Tcf4, CamkII, GDF11[41,42], and other previously reported molecular biomarkers of depression or potential therapeutic targets. Recent evidence suggests that miR-10a, miR-19b, miR-96, miR-135a, miR-139, miR-218, miR-342, miR-370, miR-383, and let-7b play important roles in depression. For example, the expression of miR-10a and let-7b in MDD patients is markedly lower than that in healthy controls, while antidepressant treatment has been shown to significantly increase miR-10a levels[43,44]. MiR-19b and miR-218 serve as key epigenetic regulators that may influence anxiety disorders through their interactions with MAPK signaling[45]. MiR-139-5p in the exosomes of MDD patients mediates neurogenesis to induce significant depressive behaviors in mice[46]. MiR-135a is downregulated by earlylife stress in female rats and is abrogated by URB597[47]. Our sequencing data revealed that HPC effectively regulated the above DEmiRNAs in restraint stress model mice. In particular, the predicted target genes of these DEmiRNAs overlapped with the previously mentioned DEmRNAs, forming regulatory pairs such as miR-10a-5p-Kalirin, miR-135a-5p-Grm5, miR-139-5p-Bcl2, miR-218-1-3p-Picalm, miR-370-3p-Ubtf, miR-383-3p-Slc1a2, and let-7b-5p-Hrh1 (Fig. 10a), highlighting their crucial role in the antidepressant mechanism of HPC.

The limited number of relevant studies has resulted in a lack of understanding regarding the functions of the majority of identified DElncRNAs and DEcircRNAs in HPC and depression. Nonetheless, several publications have validated the roles of individual DElncRNAs and DEcircRNAs. For example, the lncRNA Six3os1 mediates histone methylation to influence BDNF expression, contributing to the pathophysiology of depression by impacting oxidative stress and neuronal damage[48]. The downregulation of lncRNA GAS5 activates the PI3-K/Akt pathway via the miR-26a/EGR1 axis, thereby alleviating neuronal damage in mice exhibiting depression-like symptoms[49]. Furthermore, the circRNA HECW2 is implicated in astrocyte dysfunction and depression-like behaviors in CUMS mice through its regulation of mA methylation[50]. However, the sequencing results suggested a potential mechanism whereby DElncRNAs and DEcircRNAs function as miRNAs sponges during HPC intervention in depression, as indicated by regulatory pairs such as lncRNA ENSMUST00000247446-miR-96-5p, lncRNA XR_004942117.1-miR-139-5p, lncRNA 6_54302651_54327341-miR-135a-5p, lncRNA 7_142544608_142558598-miR-383-3p, lncRNA 2_91032191_91053934- miR-342-3p, circ_7_19170863_19171443-miR-19b-1-5p, circ_3_152232355_152,321,686-miR-383-3p, and circ_3_122575216_122611716-miR-342-3p.

Moreover, studies support the importance of the ceRNA mechanism in depression and its potential as a target for therapeutic drug development[51]. The ceRNA networks were constructed and explored in the context of depression treatment with Meranzin hydrate[52] and Xiaoyaosan[53]. Accordingly, on the basis of DERNAs, we also created ceRNA networks to elucidate their impact on the treatment of depression with HPC (Fig. 10). In the lncRNA-miRNA-mRNA network, lncRNA XR_004942117.1 served as a sponge for miR-139-5p and miR-3102-3p.2-3p, regulating the target genes Bcl2 and Picalm, whereas lncRNA 6_54302651_54327341 acted as a sponge for miR-135a-5p and miR-7689-3p to regulate Grm5 and Cacna1a (Fig. 10b). In the circRNA-miRNA-mRNA network, circ_3_122575216_122611716 functions as a sponge for miR-342-3p and miR-216a-5p to regulate Ubtf and Plch1, and circ_3_58938967_59001116 functions as a sponge for miR-216a-5p and miR-217-5p, regulating Plch1 and Camk2a (Fig. 10c). Furthermore, miR-383-3p was centrally located and interacted with 6 DElncRNAs and 3 DEcircRNAs in our ceRNA network, indicating that these molecules might be key regulatory molecules for the antidepressant effects of HPC. Studies have shown that the inhibition of miR-383, which is overexpressed in a rat CUMS model, may upregulate BDNF, GFAP, and CREB expression to reduce the apoptosis and inflammation of hippocampal neurons, ultimately diminishing depression-like behaviors[54]. Our sequencing data also revealed that HPC downregulated miR-383-3p in restraint stress model mice and predicted Slc1a2 as a target gene, and Slc1a2 was strongly associated with depression[55]. In summary, our analysis exhibited the considerable potential of ceRNA networks composed of DERNAs in alleviating depression-like behaviors with HPC. In particular, we will regard miR-383-3p as a key factor in HPC intervention in depression through a ceRNA mechanism for further research.

GO and KEGG enrichment analyses uncovered that the enriched biological processes in the DERNAs were predominantly axons, dendrites, synapses, and neurogenesis, along with related processes such as transmembrane transport, protein binding, and transcription coregulator binding (Figs. 9a–d and 11a), all of which are well-established pathophysiologies implicated in depression. Downstream BDNF signaling pathways, such as the MAPK pathway, phosphatidylinositol pathway, cAMP pathway, mTOR pathway and neurotrophin signaling, were the main enriched pathways (Figs. 9e–h and 11b). Our experimental results, corroborated by previous studies, consistently demonstrated that BDNF signaling is a highly effective target for HPC neuroprotection and the treatment of depression. Overall, we propose that the HPC influences depression potentially through a multitude of pathways that may ameliorate abnormalities in synaptic function and neurogenesis. Importantly, the limited sample size and the choice of mouse model for simulating depression-like behaviors prevented the identification of DEncRNAs that directly regulate BDNF expression using whole transcriptome sequencing. Nonetheless, the direct target genes of these DEncRNAs and DEmRNAs encompassed numerous critical factors involved in BDNF signaling downstream, which also engaged in the regulation of BDNF signaling and its responsible synaptic function and neurogenesis. Therefore, the HPC might combat depression by facilitating neuronal synapses and neurogenesis through the combined action of ncRNAs and BDNF signaling indirectly regulated by ncRNAs.

Conclusion

In conclusion, our study revealed that HPC downregulated BDNF expression and activated BDNF/PLCγ/CREB signaling in the mouse hippocampus, thereby ameliorating synaptic structural deficits, promoting neurogenesis, and ultimately alleviating depression-like behaviors in mice. In addition, we identified and analyzed multiple DElncRNAs, DEcircRNAs, DEmiRNAs, and DEmRNAs in hippocampal tissues before and after HPC treatment in restraint stress model mice via whole transcriptome sequencing. Moreover, ceRNA networks were constructed to further explore the antidepressant mechanism of HPC. These findings provide new insights into the molecular

mechanisms through which HPC improves depression-like behaviors and establish a theoretical foundation for its clinical application in the treatment of depression.

Data availability

The experimental data used to support the findings of this study are available from the Figshare (Chen, Lizhu; Wang, Xujie; Jia, Xiaoe; Bade, Rengui; Liu, Xiaolei; Jiang, Shuyuan; et al. (2025). Hypoxic Preconditioning Modulates BDNF Signaling to Alleviate Depression-like Behaviors in Mice and Its Whole Transcriptome Sequencing Analysis. figshare. Dataset. https://doi.org/10.6084/m9.figshare.28510994.v1). The whole transcriptome sequencing datasets generated and analysed during the current study are available in the NCBI Sequence Read Archive (SRA) repository, accession number PRJNA1210851 (http://www.ncbi.nlm.nih.gov/bioproject/1210851), and BioSample accessions SAMN46258684 (https://www.ncbi.nlm.nih.gov/biosample/46258684), SAMN46258685 (https://www.ncbi.nlm.nih.gov/biosample/46258685), SAMN46258686 (https://www.ncbi.nlm.nih.gov/biosample/46258686), SAMN46258687 (https://www.ncbi.nlm.nih.gov/biosample/46258687), SAMN46258688 (https://www.ncbi.nlm.nih.gov/biosample/46258688), SAMN46258689 (https://www.ncbi.nlm.nih.gov/biosample/46258689). The animals and detailed reagents and methodological procedures used to support the experimental study are available from the corresponding author upon request.

Received: 10 January 2025; Accepted: 28 April 2025
Published online: 02 May 2025

References

1. Marx, W. et al. Major depressive disorder. *Nat. Reviews Disease Primers*. **9** (1), 44. https://doi.org/10.1038/s41572-023-00454-1 (2023).
2. Dwyer, J. B. et al. Hormonal treatments for major depressive disorder: state of the Art. *Am. J. Psychiatry*. **177** (8), 686–705. https://doi.org/10.1176/appi.ajp.2020.19080848 (2020).
3. Patil, C. R., Suryakant Gawli, C. & Bhatt, S. Targeting inflammatory pathways for treatment of the major depressive disorder. *Drug Discovery Today*. **28** (9), 103697. https://doi.org/10.1016/j.drudis.2023.103697 (2023).
4. Bian, Z. et al. The association between hypoxia improvement and electroconvulsive therapy for major depressive disorder. *Neuropsychiatr. Dis. Treat.* **17**, 2987–2994. https://doi.org/10.2147/NDT.S318919 (2021).
5. Lu, G. W. & Shao, G. Hypoxic preconditioning: effect, mechanism and clinical implication (Part 1). Zhongguo Ying Yong Sheng Li Xue Za zhi = zhongguo Yingyong Shenglixue Zazhi = Chinese. *J. Appl. Physiol.* **30** (6), 489–501 (2014).
6. Shao, G. & Lu, G. W. Hypoxic preconditioning in an autohypoxic animal model. *Neurosci. Bull.* **28** (3), 316–320. https://doi.org/10.1007/s12264-012-1222-x (2012).
7. Shi, Y., Wang, Q., Song, R., Kong, Y. & Zhang, Z. Non-coding RNAs in depression: promising diagnostic and therapeutic biomarkers. *EBioMedicine* **71**, 103569. https://doi.org/10.1016/j.ebiom.2021.103569 (2021).
8. Garcia-Gutierrez, M. S. et al. Alterations of BDNF, mGluR5, Homer1a, p11 and excitatory/inhibitory balance in corticolimbic brain regions of suicide decedents. *J. Affect. Disord.* **339**, 366–376. https://doi.org/10.1016/j.jad.2023.07.003 (2023).
9. Wang, Z. et al. Safety and tolerability of both arm ischemic conditioning in patients with major depression: A proof of concept study. *Front. Psychiatry*. **11**, 570. https://doi.org/10.3389/fpsyt.2020.00570 (2020).
10. Jafarabady, K. et al. Brain-derived neurotrophic factor levels in perinatal depression: A systematic review and meta-analysis. *Acta Psychiatry. Scand.* https://doi.org/10.1111/acps.13632 (2023).
11. Szuhany, K. L. & Simon, N. M. Anxiety disorders: A review. *Jama* **328** (24), 2431–2445. https://doi.org/10.1001/jama.2022.22744 (2022).
12. Zhang, S. et al. Hypoxic preconditioning modulates BDNF and its signaling through DNA methylation to promote learning and memory in mice. *ACS Chem. Neurosci.* **14** (12), 2320–2332. https://doi.org/10.1021/acschemneuro.3c00069 (2023).
13. Wang, Y. et al. TrkB/BDNF signaling pathway and its small molecular agonists in CNS injury. *Life Sci.* 122282. https://doi.org/10.1016/j.lfs.2023.122282 (2023).
14. Cubillos, S., Engmann, O. & Brancato, A. BDNF as a mediator of antidepressant response: recent advances and lifestyle interactions. *Int. J. Mol. Sci.* **23** (22). https://doi.org/10.3390/ijms232214445 (2022).
15. Chen, H. S., Wang, F. & Chen, J. G. Epigenetic mechanisms in depression: implications for pathogenesis and treatment. *Curr. Opin. Neurobiol.* **85**, 102854. https://doi.org/10.1016/j.conb.2024.102854 (2024).
16. Abdolahi, S., Zare-Chahoki, A., Noorbakhsh, F. & Gorji, A. A review of molecular interplay between neurotrophins and MiRNAs in neuropsychological disorders. *Mol. Neurobiol.* **59** (10), 6260–6280. https://doi.org/10.1007/s12035-022-02966-5 (2022).
17. Chu, X. et al. 24-hour-restraint stress induces long-term depressive-like phenotypes in mice. *Sci. Rep.* **6**, 32935. https://doi.org/10.1038/srep32935 (2016).
18. Kanehisa, M., Furumichi, M., Sato, Y., Matsuura, Y. & Ishiguro-Watanabe, M. KEGG: biological systems database as a model of the real world. *Nucleic Acids Res.* **53** (D1), D672–D677. https://doi.org/10.1093/nar/gkae909 (2025).
19. Kanehisa, M. & Goto, S. KEGG: Kyoto encyclopedia of genes and genomes. *Nucleic Acids Res.* **28** (1), 27–30. https://doi.org/10.1093/nar/28.1.27 (2000).
20. Burtscher, J. et al. The interplay of hypoxic and mental stress: implications for anxiety and depressive disorders. *Neurosci. Biobehav. Rev.* **138**, 104718. https://doi.org/10.1016/j.neubiorev.2022.104718 (2022).
21. Li, S. et al. Hamartin: an endogenous neuroprotective molecule induced by hypoxic preconditioning. *Front. Genet.* **11**, 582368. https://doi.org/10.3389/fgene.2020.582368 (2020).
22. Kramer, B. A. et al. Exercise elevates serum brain-derived neurotrophic factor in partially remitted depression. *Psychiatry Res.* **326**, 115283. https://doi.org/10.1016/j.psychres.2023.115283 (2023).
23. Kushwah, N. et al. Neuroprotective role of intermittent hypobaric hypoxia in unpredictable chronic mild stress induced depression in rats. *PloS One*. **11** (2), e0149309. https://doi.org/10.1371/journal.pone.0149309 (2016).
24. Li, S. et al. Preconditioning in neuroprotection: from hypoxia to ischemia. *Prog. Neurobiol.* **157**, 79–91. https://doi.org/10.1016/j.pneurobio.2017.01.001 (2017).
25. Lu, G. W., Yu, S., Li, R. H., Cui, X. Y. & Gao, C. Y. Hypoxic preconditioning: a novel intrinsic cytoprotective strategy. *Mol. Neurobiol.* **31** (1–3), 255–271. https://doi.org/10.1385/MN:31:1-3:255 (2005).
26. Yao, Y. et al. High-intensity interval training ameliorates postnatal immune activation-induced mood disorders through KDM6B-regulated glial activation. *Brain. Behav. Immun.* **120**, 290–303. https://doi.org/10.1016/j.bbi.2024.06.006 (2024).
27. Wang, X. et al. High-frequency repetitive transcranial magnetic stimulation improves depressive-like behaviors in CUMS-induced rats by modulating astrocyte GLT-1 to reduce glutamate toxicity. *J. Affect. Disord.* **348**, 265–274. https://doi.org/10.1016/j.jad.2023.12.068 (2024).

28. Shashikumara, S., Purushotham, K., Darshan, C. L. & Kalal, B. S. Characterization of antidepressant activity of Saraca Asoca flower (Roxb.) Wilde in mice subjected to acute restraint stress. *Am. J. Translational Res.* **14** (7), 5014–5023 (2022).
29. Thakare, V. N., Dhakane, V. D. & Patel, B. M. Attenuation of acute restraint stress-induced depressive like behavior and hippocampal alterations with Protocatechuic acid treatment in mice. *Metab. Brain Dis.* **32** (2), 401–413. https://doi.org/10.1007/s11011-016-9922-y (2017).
30. Erbay, L. G., Karlidag, R., Oruc, M., Cigremis, Y. & Celbis, O. Association of BDNF / TrkB and NGF / TrkA levels in postmortem brain with major depression and suicide. *Psychiatria Danubina*. **33** (4), 491–498. https://doi.org/10.24869/psyd.2021.491 (2021).
31. Cavaleri, D. et al. The role of BDNF in major depressive disorder, related clinical features, and antidepressant treatment: insight from meta-analyses. *Neurosci. Biobehav. Rev.* **149**, 105159. https://doi.org/10.1016/j.neubiorev.2023.105159 (2023).
32. Shirayama, Y., Chen, A. C., Nakagawa, S., Russell, D. S. & Duman, R. S. Brain-derived neurotrophic factor produces antidepressant effects in behavioral models of depression. *J. Neuroscience: Official J. Soc. Neurosci.* **22** (8), 3251–3261 (2002). doi:20026292.
33. Zeng, J. et al. Rosmarinic acid alleviate CORT-induced depressive-like behavior by promoting neurogenesis and regulating BDNF/TrkB/PI3K signaling axis. *Biomed. Pharmacotherapy = Biomedecine Pharmacotherapie*. **170**, 115994. https://doi.org/10.1016/j.biopha.2023.115994 (2024).
34. Yang, Y. R. et al. Forebrain-specific ablation of phospholipase Cgamma1 causes manic-like behavior. *Mol. Psychiatry*. **22** (10), 1473–1482. https://doi.org/10.1038/mp.2016.261 (2017).
35. Ji, C. H. et al. Hippocampal MSK1 regulates the behavioral and biological responses of mice to chronic social defeat stress: involving of the BDNF-CREB signaling and neurogenesis. *Biochem. Pharmacol.* **195**, 114836. https://doi.org/10.1016/j.bcp.2021.114836 (2022).
36. Liaqat, H., Parveen, A. & Kim, S. Y. Antidepressive effect of natural products and their derivatives targeting BDNF-TrkB in Gut-Brain Axis. *Int. J. Mol. Sci.* **23** (23). https://doi.org/10.3390/ijms232314968 (2022).
37. Numakawa, T. & Kajihara, R. Involvement of brain-derived neurotrophic factor signaling in the pathogenesis of stress-related brain diseases. *Front. Mol. Neurosci.* **16**, 1247422. https://doi.org/10.3389/fnmol.2023.1247422 (2023).
38. Cui, J. et al. Exosomal MicroRNA-126 from RIPC serum is involved in hypoxia tolerance in SH-SY5Y cells by downregulating DNMT3B. *Mol. Therapy Nucleic Acids*. **20**, 649–660. https://doi.org/10.1016/j.omtn.2020.04.008 (2020).
39. Liu, N. et al. Neuroprotective mechanisms of DNA methyltransferase in a mouse hippocampal neuronal cell line after hypoxic preconditioning. *Neural Regeneration Res.* **15** (12), 2362–2368. https://doi.org/10.4103/1673-5374.285003 (2020).
40. Zhang, P. et al. Up-regulation of miR-126 via DNA methylation in hypoxia-preconditioned endothelial cells May contribute to hypoxic tolerance of neuronal cells. *Mol. Biol. Rep.* **51** (1), 808. https://doi.org/10.1007/s11033-024-09774-1 (2024).
41. Howard, D. M. et al. Genome-wide meta-analysis of depression identifies 102 independent variants and highlights the importance of the prefrontal brain regions. *Nat. Neurosci.* **22** (3), 343–352. https://doi.org/10.1038/s41593-018-0326-7 (2019).
42. Kukulowicz, J., Pietrzak-Lichwa, K., Klimonczyk, K., Idlin, N. & Bajda, M. The SLC6A15-SLC6A20 neutral amino acid transporter subfamily: functions, diseases, and their therapeutic relevance. *Pharmacol. Rev.* **76** (1), 142–193. https://doi.org/10.1124/pharmrev.123.000886 (2023).
43. Liu, W. et al. The role of Circulating blood microRNA-374 and microRNA-10 levels in the pathogenesis and therapeutic mechanisms of major depressive disorder. *Neurosci. Lett.* **763**, 136184. https://doi.org/10.1016/j.neulet.2021.136184 (2021).
44. Gururajan, A. et al. MicroRNAs as biomarkers for major depression: a role for let-7b and let-7c. *Translational Psychiatry*. **6** (8), e862. https://doi.org/10.1038/tp.2016.131 (2016).
45. Amini, J., Beyer, C., Zendedel, A. & Sanadgol, N. MAPK is a mutual pathway targeted by Anxiety-Related MiRNAs, and E2F5 is a putative target for anxiolytic MiRNAs. *Biomolecules* **13** (3). https://doi.org/10.3390/biom13030544 (2023).
46. Wei, Z. X. et al. Exosomes from patients with major depression cause depressive-like behaviors in mice with involvement of miR-139-5p-regulated neurogenesis. *Neuropsychopharmacology: Official Publication Am. Coll. Neuropsychopharmacol.* **45** (6), 1050–1058. https://doi.org/10.1038/s41386-020-0622-2 (2020).
47. Portugalov, A., Zaidan, H., Gaisler-Salomon, I., Hillard, C. J. & Akirav, I. FAAH Inhibition restores early life Stress-Induced alterations in PFC MicroRNAs associated with Depressive-Like behavior in male and female rats. *Int. J. Mol. Sci.* **23** (24). https://doi.org/10.3390/ijms232416101 (2022).
48. Zou, T. et al. Zhi-zi-chi Decoction mitigates depression by enhancing LncRNA Six3os1 expression and promoting histone H3K4 methylation at the BDNF promoter. *J. Cell. Mol. Med.* **28** (11), e18365. https://doi.org/10.1111/jcmm.18365 (2024).
49. Wu, Y., Rong, W., Jiang, Q., Wang, R. & Huang, H. Downregulation of LncRNA GAS5 alleviates hippocampal neuronal damage in mice with Depression-Like behaviors via modulation of MicroRNA-26a/EGR1 Axis. *J. Stroke Cerebrovasc. Diseases: Official J. Natl. Stroke Association*. **30** (3), 105550. https://doi.org/10.1016/j.jstrokecerebrovasdis.2020.105550 (2021).
50. Bai, Y. et al. Engagement of N(6)-methyladenisine methylation of Gng4 mRNA in astrocyte dysfunction regulated by CircHECW2. *Acta Pharm. Sinica B*. **14** (4), 1644–1660. https://doi.org/10.1016/j.apsb.2024.01.011 (2024).
51. Liao, W. et al. Intersectional analysis of chronic mild stress-induced lncRNA-mRNA interaction networks in rat hippocampus reveals potential anti-depression/anxiety drug targets. *Neurobiol. Stress*. **15**, 100347. https://doi.org/10.1016/j.ynstr.2021.100347 (2021).
52. Nie, K. et al. Effects of Meranzin hydrate on the LncRNA-miRNA-mRNA regulatory network in the Hippocampus of a rat model of depression. *J. Mol. Neuroscience: MN*. **72** (4), 910–922. https://doi.org/10.1007/s12031-022-01971-6 (2022).
53. Meng, P. et al. A whole transcriptome profiling analysis for antidepressant mechanism of Xiaoyaosan mediated synapse loss via BDNF/trkB/PI3K signal axis in CUMS rats. *BMC Complement. Med. Ther.* **23** (1), 198. https://doi.org/10.1186/s12906-023-04000-0 (2023).
54. Liu, S., Liu, Q., Ju, Y. & Liu, L. Downregulation of miR-383 reduces depression-like behavior through targeting Wnt family member 2 (Wnt2) in rats. *Sci. Rep.* **11** (1), 9223. https://doi.org/10.1038/s41598-021-88560-6 (2021).
55. Liu, Y. et al. Unveiling the hidden pathways: exploring astrocytes as a key target for depression therapy. *J. Psychiatr. Res.* **174**, 101–113. https://doi.org/10.1016/j.jpsychires.2024.04.003 (2024).

Author contributions

Origination of research ideas and writing of drafts: WX and MHG. Animal and molecular biology experiments: LZC. Whole transcriptome sequencing and bioinformatics analysis: XJW and RGBD. Design of experimental methods: WX, MHG, GS and XEJ. Process and statistical analysis of experimental data:, YBX, SYJ and XLL. Submission and revised the manuscript: WX, MHG and GS. LZC and XJW contributed equally to this work. All authors reviewed the manuscript.

Funding

This research was funded by support from the National Natural Science Foundation of China (82071479 and 31860307 to WX), the Young Innovative and Entrepreneurial Talents of the 'Grassland Talents' Project in Inner Mongolia Autonomous Region (to WX), the Projects of Scientific Research of Higher Education Institutions in Inner Mongolia Autonomous Region (NJZY23094 to MHG), the Baotou Medical College Innovation Team Development Plan Project (bycxtd-12 to WX).

Declarations

Competing interests
The authors declare no competing interests.

Ethical approval
All methods were carried out in accordance with the guidelines of National Institutes of Health and the Medical Ethics Review Committee of Baotou Medical College, and were approved by the Medical Ethics Review Committee of Baotou Medical College (approval numbers: 2021034. April 19, 2021). All experimental methods were conducted in accordance with the ARRIVE guidelines. All methods were carried out in accordance with relevant guidelines and regulations.

Additional information
Supplementary Information The online version contains supplementary material available at https://doi.org/10.1038/s41598-025-00355-1.

Correspondence and requests for materials should be addressed to W.X. or M.G.

Reprints and permissions information is available at www.nature.com/reprints.

Publisher's note Springer Nature remains neutral with regard to jurisdictional claims in published maps and institutional affiliations.